Inhomogeneous plane-wave scattering and mode stimulation on periodic rough surfaces

Koen E.-A. Van Den Abeele,[a] Rudy Briers, and Oswald Leroy
IRC, K.U. Leuven Campus Kortrijk, B-8500 Kortrijk, Belgium

(Received 1 August 1995; accepted for publication 23 December 1995)

Medium vibration properties to characterize interface layers and quality of bonding can be examined by an ordinary approach using homogeneous waves or by a more general inhomogeneous (or complex harmonic) wave scattering technique. It is known that only particular inhomogeneous plane waves can stimulate eigenvibrations of a given structure, and not the homogeneous wave. The reflection and transmission of such inhomogeneous waves is investigated for plane parallel interfaces as well as their scattering at periodically corrugated boundaries between liquid and solids. The influence of plate thickness, corrugation periodicity, and height on the occurrence of specific plate modes is examined. Using an alternative description of a bounded ultrasonic beam as a finite superposition of inhomogeneous waves, this theory can be applied to examine the deformation of Gaussian profiles and to explicitly relate this deformation to the stimulation of mode vibrations. The generation of a plate—or interface—mode by an obliquely incident single inhomogeneous wave on a plane parallel plate—or half-space interface boundary—and the scattering of inhomogeneous waves at the interface wave stimulated corrugated surface, also suggest a new interpretation of back reflection and transmission of bounded beams at smooth liquid–solid interfaces.

PACS numbers: 43.35.Pt

INTRODUCTION

Although most attention is usually focused on classical plane homogeneous waves, inhomogeneous waves, with an exponentially decaying amplitude (represented by the parameter β) along the plane-wave front, are the most general solution of the wave equation for a homogeneous and isotropic linearly viscoelastic material. These waves are also often called heterogeneous waves or complex harmonic waves because of their theoretical description by means of a complex valued wave vector.[1–3] On the other hand, the mathematical representation of any type of surface wave (leaky Lamb or Rayleigh waves and Stoneley waves) is locally a combination of such heterogeneous waves and cannot be described in terms of homogeneous waves.[4] Therefore it may not seem surprising at all that (in general) only inhomogeneous waves are the real stimuli of material vibrations.

In this work we focus on the excitation of surface waves as a consequence of bulk ultrasonic wave interaction with periodic rough surfaces. This topic has been studied in detail by quite a number of scientific groups employing a large variety of approximations. We refer the reader to the introduction and review of Bishop and Smith[5] and to the book of Maystre[6] for a detailed overview of all methods used to study diffraction gratings and for a nearly complete list of the most important references on this subject. A survey of the literature immediately brings to light that most of the theoretical and experimental reports deal with the case of incident plane homogeneous waves. However, in recent years we have been convinced both by theoretical and experimental evidence that a study of complex harmonic waves generally reveals much more information about the scanned medium.[3,7–9] Therefore we generalized the scattering model to account for bulk inhomogeneous plane-waves incident on periodic rough surfaces. We use the oldest and simplest technique to calculate scattering from a periodic surface as developed by Rayleigh,[10] realizing very well that this hypothesis has been a subject of controversy since the early 1950s.[11–14] Strikingly enough, none of the more advanced theoretical approaches seems to agree on the exact limits of validation of the Rayleigh hypothesis (see Ref. 5 for a discussion). Qualitatively, the assumptions are believed to be valid in cases where the wavelength of the incident sound beam is of the same order of magnitude as the periodicity and much larger than the depth of the grating.

We start with the case of plane parallel interfaces and illustrate the importance of complex harmonic waves in connection with plate mode stimulation (Sec. I A). Next, we study the case of a plate with a periodically corrugated surface at the top and a plane interface at the bottom. The scattering process is established due to the periodic boundary conditions at the top surface. In this paper we limit our study to normal incidence. We will show that the anomalies in the amplitudes of the diffraction orders can be explained as particular conditions for eigenvibrations of the structure. We will not consider other anomalies such as Brewster angle anomalies and Wood P anomalies, which occur as a consequence of the behavior of the modal spectrum of the rough surface rather than being produced by excitation of the structure eigenvibrations. We refer the reader to the work of DeSanto for that manner.[15] The location of eigenvibrations for the corrugated specimen can be deduced from the dispersion curves of a sample with plane parallel interfaces. Just as for

[a]Postdoctoral fellow of the Belgian National Fund for Scientific Research. Presently at EES-4, MS D443, Los Alamos National Laboratory, Los Alamos, New Mexico 87545.

 0001-4966/96/99(5)/2883/15/$6.00

the smooth plate, we find that the inhomogeneous plane waves are the real stimuli of eigenvibrations, not the homogeneous plane waves. We illustrate this for several Lamb modes in a corrugated plate (Sec. I B) and for Rayleigh and Stoneley resonances at a corrugated interface between half-spaces (Sec. II). In Sec. III, we investigate the influence of plate thickness and corrugation profile (shape, periodicity, and height) on the resonance characteristics of a particular mode. We also point out some independence relations that can be important for scaling problems to laboratory research models. Section IV deals with bounded beam scattering on periodic rough surfaces. We use a previously reported alternative description of a bounded beam in terms of a finite number of inhomogeneous plane waves[7–8] to explicitly relate beam deformation to the generation of plate/interface waves. The scattering properties of complex harmonic waves can be applied to investigate symmetry conditions, beamwidth influence, and multiple mode occurrences. Finally, in Sec. V, we launch an alternative concept for the physical mechanism that leads to the observation of backscattering (backreflection and backtransmission) when bounded beams interact with plane parallel plates.[16–19] The idea is based on inhomogeneous wave mode stimulation in combination with scattering from a self-supported corrugated surface.

I. SCATTERING FROM A SOLID PLATE IMMERSED IN A LIQUID

A. Plane parallel interfaces

The dispersion curves for a 2-mm-brass plate with plane parallel interfaces immersed in water are given in Fig. 1, calculated using the following medium parameters:

Water: longitudinal velocity: $\nu_l = 1480$ m/s;
attenuation: $a_l\omega^2 = 4\times10^{-8}$ Np/mm at 1 MHz with $\omega = 2\pi f$;
density: 1000 kg/mm^3.

Brass: dilatational velocity: $\nu_d = 4840$ m/s;
dilatational attenuation: $a_d\omega^2 = 4\times10^{-6}$ Np/mm at 1 MHz;
shear velocity: $\nu_s = 2270$ m/s;
shear attenuation: $a_s\omega^2 = 2\times10^{-5}$ Np/mm at 1 MHz;
density: 8100 kg/mm^3.

Let f be the frequency, θ_{inc} the angle of incidence, and ν_m the mode velocity along the surface. From a theoretical point of view, the dispersion curves correspond to the ''f-θ_{inc}'' combinations or equivalently ''f-ν_m'' combinations for which the denominator of the reflection coefficient of a plane wave vanish. Expressions for the reflection and transmission coefficients can be found in many textbooks.[4,20,21] The zero's correspond to two families of modes: symmetric (S) and asymmetric (A) modes. We notice that five different mode singularities can be obtained for different angles of incidence at a frequency of 1.5 MHz: A_0, S_0, A_1, S_1, and S_2 (circles in Fig. 1). The interpretation is that each singularity represents a vibration of the solid layer that propagates laterally inside the plate. In addition, a singularity occurs at the Stoneley wave velocity (1478 m/s for water/brass systems), corresponding to an angle of incidence parallel to the interface (square in Fig. 1). In contrast to the other five modes the

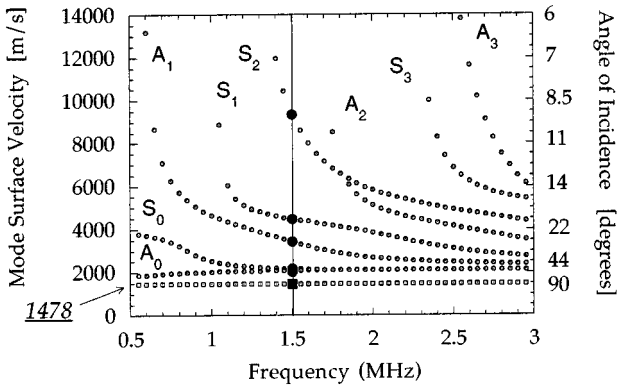

FIG. 1. Dispersion curves for a smooth 2-mm-thick brass plate immersed in water. The vertical axis on the right-hand side corresponds to the angle of incidence for which plate modes are generated using bounded beams. The scale is not linear as the values on this axis correspond to ArcSin (1480.0/mode velocity).

displacement of the Stoneley mode is mostly located in the liquid. All these modes are so-called eigenmodes of the liquid–solid–liquid system and thus exist permanently. They can be stimulated under certain circumstances, analogous to the resonance of a spring at forced oscillation.

The reflection coefficient (in dB) as a function of the incidence angle (-50–$+50$ deg) for a *homogeneous* wave at 1.5 MHz is visualized in Fig. 2(a). For each mode one observes a sharp dip in the reflection coefficient. Although these null positions are often interpreted as stimulations of the eigenmodes of the system, this interpretation is incorrect. Stimulation of a particular eigenmode does not happen when the reflection coefficient vanishes. Since the zeroes of the denominator of the reflection coefficient represent complex wave numbers, stimulation occurs only for incident *inhomogeneous waves*, often also called heterogeneous or complex harmonic waves. In order to substantiate this statement we plotted in the same figure the reflection moduli for specific inhomogeneous waves. The parameter β_{inc} in Fig. 2(b)–(f) is related to the imaginary part of the wave number at the singularity and corresponds to the heterogeneity parameter (exponential decay of the wave profile along the wavefront) characteristic for a complex harmonic wave. (For a complete description of an inhomogeneous plane wave, see Refs. 1–3 and 7–9.) We observe that the modulus of the reflection coefficient exhibits a maximum at the mode positions of S_2, S_1, A_1, S_0, and A_0 for certain particular values of the heterogeneity parameter. Note that in those circumstances the reflection modulus acquires a value much larger than unity. Moreover, in Fig. 3 we compare the displacements inside the plate for the homogeneous and the specific inhomogeneous wave that corresponds to the resonance of the A_1 mode ($f = 1.5$ MHz, $\theta_{\text{inc}} = 25.513°$). It is clear that this asymmetrical vibration is highly stimulated by the incident inhomogeneous wave with a heterogeneity parameter β_{inc} equal to -0.0651 mm^{-1}. Thus apart from frequency and angle of incidence (or mode velocity), the stimulation of vibrational modes strongly depends also on another parameter, namely, the heterogene-

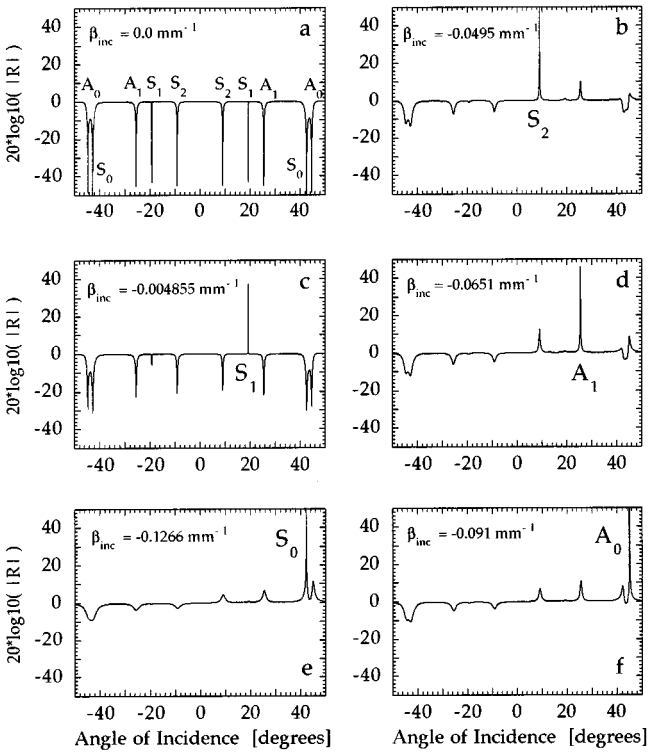

FIG. 2. Reflection coefficient (in dB) as a function of the incidence angle (in degrees) for a homogeneous plane wave (a) and particular mode stimulating inhomogeneous plane waves (b)–(f) on a 2-mm smooth brass plate at 1.5 MHz.

ity parameter β_{inc}. This is also true for half-spaces and more complicated structures.

Recently, Deschamps[9] reported the first experimental observation ever of reflection and transmission coefficients larger than unity using incident bulk inhomogeneous waves. His observations confirm theoretical predictions and form strong evidence that only inhomogeneous waves can stimulate eigenmodes in plates.

B. Periodically corrugated surfaces

The study of layered structures with plane parallel interfaces and the interaction of ultrasonic waves with materials having periodic rough surfaces have been topics of growing interest in many fields of NDT. Gratings are favorite problems for spectroscopists, but oceanographers are also interested in studying sound scattering by rough surfaces, e.g., the ocean surface. Indeed, the topic of sound scattered from periodic corrugated surfaces has been frequently examined; however, only a few studies have investigated the scattering process for inhomogeneous waves.[22,23] Most theoretical approaches and experimental reports deal with the case of incident homogeneous plane waves at normal incidence. Exactly as in the case of plane interfaces, the observed features for $\beta_{\text{inc}}=0$ at different frequencies are usually associated with the generation/stimulation of eigenmodes of the structure. This is true, but only partly, because, again, the introduction of inhomogeneous waves is required to describe exactly how these constructive interference vibrations are generated.

Figure 4 shows a scheme of the geometry for an arbitrary (upper) corrugated solid layer. The x axis ($z=0$) is chosen to be the mean of the roughness profile F. Here, h is the peak-to-peak amplitude of the surface roughness, Λ is the profile periodicity, and d is the average thickness of the layer. In this geometry the solid layer extends between $z=F(x)$ and $z=d$. We will consider the case of a general plane *inhomogeneous* wave (with exponentially decaying amplitude along its wavefront as shown in Fig. 4) incident in the x-z plane. We assume no y dependence. In this article we will limit ourselves to normal incidence. As an example we consider a 2-mm-brass plate with a corrugated upper surface (sawtooth or sine profile) and a plane boundary at the lower surface. The periodicity of the profile (Λ) is 2.2 mm and the height (h) of the corrugation is 50 mm. The brass layer is immersed in water. Since the conditions at the upper surface are periodic along that interface, it is assumed that the mathematical solution of the (inhomogeneous) reflected and transmitted ultrasonic fields, as well as the (inhomogeneous) longitudinal and shear waves propagating inside the plate, can be represented by a Fourier series in the coordinate along the interface. This means that the incident energy will be scattered in several plane inhomogeneous waves having different

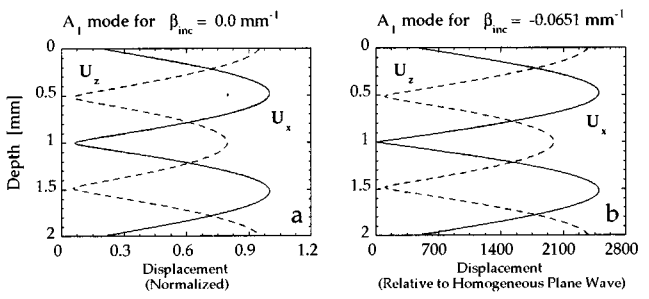

FIG. 3. Relative A_1 displacement components inside a 2-mm brass plate generated at 1.5 MHz for incidence angle $\theta_{\text{inc}}=26.07°$ by (a) a homogeneous plane wave ($\beta_{\text{inc}}=0.0\ \text{mm}^{-1}$), (b) the A_1 mode stimulating inhomogeneous plane wave ($\beta_{\text{inc}}=-0.0651\ \text{mm}^{-1}$).

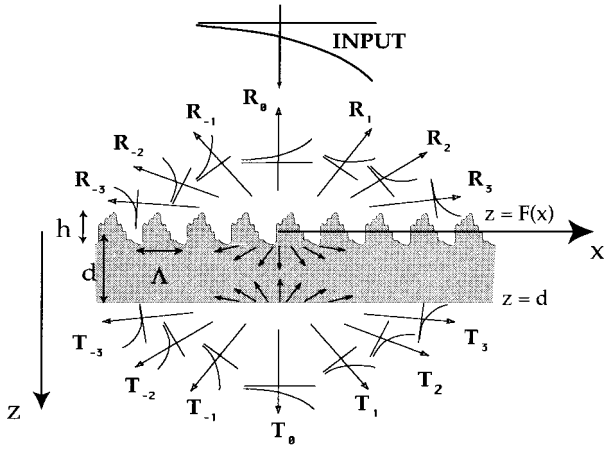

FIG. 4. Geometry of the two-dimensional diffraction problem for inhomogeneous plane waves at normal incidence.

directions in reflection and transmission. Also, inside the plate different orders will be generated which travel with different group velocity projections along the interface. This assumption corresponds to Rayleigh's basic idea[10] and although its validity is questioned by many scientists,[11–14] its simplicity opens perspectives for a straightforward understanding of the physics behind the problem.

Following a similar theoretical treatment for solid–vacuum,[22] liquid–solid,[24] or solid–liquid[25] half-space interfaces, the system of linear equations that result from the implementation of the six boundary conditions for the reflected, transmitted, and in-plate generated waves, can be written as follows:

$$\sum_{m=-\infty}^{+\infty}[k_m k_n-\kappa_l^2]R_m I_{mn}^r+\sum_{m=-\infty}^{+\infty}[\kappa_d^2-k_m k_n]\times(D_m^+ I_{mn}^{d+}+D_m^- I_{mn}^{d-})+\sum_{m=-\infty}^{+\infty}k_n K_{sm}(S_m^+ I_{mn}^{s+}-S_m^- I_{mn}^{s-})=[\kappa_l^2-k_x^{\rm inc}k_n]I_{0n}, \tag{1a}$$

$$\sum_{m=-\infty}^{+\infty}[k_m-k_n]R_m I_{mn}^r-\rho\sum_{m=-\infty}^{+\infty}[k_m-k_n+2k_n K_{dm}^2/\kappa_s^2]\times(D_m^+ I_{mn}^{d+}+D_m^- I_{mn}^{d-})+\rho\sum_{m=-\infty}^{+\infty}K_{sm}[1-2k_m k_n/\kappa_s^2]\times(S_m^+ I_{mn}^{s+}-S_m^- I_{mn}^{s-})=[k_n-k_x^{\rm inc}]I_{0n}, \tag{1b}$$

$$\sum_{m=-\infty}^{+\infty}K_{rm}R_m I_{mn}^r-\rho\sum_{m=-\infty}^{+\infty}K_{dm}[1-2k_m k_n/\kappa_s^2](D_m^+ I_{mn}^{d+}-D_m^- I_{mn}^{d-})-\rho\sum_{m=-\infty}^{+\infty}[k_m-k_n+2k_n K_{sm}^2/\kappa_s^2]\times(S_m^+ I_{mn}^{s+}+S_m^- I_{mn}^{s-})=-K_{\rm inc}I_{0n}, \tag{1c}$$

$$\sum_{m=-\infty}^{+\infty}K_{dm}(D_m^+ J_{mn}^{d+}-D_m^- J_{mn}^{d-})+\sum_{m=-\infty}^{+\infty}k_m(S_m^+ J_{mn}^{s+}+S_m^- J_{mn}^{s-})-\sum_{m=-\infty}^{+\infty}K_{tm}T_m J_{mn}^{t+}=0, \tag{1d}$$

$$2\sum_{m=-\infty}^{+\infty}k_m K_{dm}(D_m^+ J_{mn}^{d+}-D_m^- J_{mn}^{d-})+\sum_{m=-\infty}^{+\infty}[2k_m^2-\kappa_s^2]\times(S_m^+ J_{mn}^{s+}+S_m^- J_{mn}^{s-})=0, \tag{1e}$$

$$\rho\sum_{m=-\infty}^{+\infty}[1-2k_m^2/\kappa_s^2](D_m^+ J_{mn}^{d+}+D_m^- J_{mn}^{d-})+\rho\sum_{m=-\infty}^{+\infty}2k_m K_{sm}/\kappa_s^2(S_m^+ J_{mn}^{s+}-S_m^- J_{mn}^{s-})-\sum_{m=-\infty}^{+\infty}T_m J_{mn}^{t+}=0, \tag{1f}$$

with n ranging from $-\infty$ to $+\infty$. Here, R_m, T_m, D_m^+, D_m^-, S_m^+, and S_m^- are the unknown reflection, transmission, and up- and downgoing dilatational and shear wave coefficients; ρ is the ratio of solid density to liquid density; κ_l, κ_d, and κ_s are complex-valued medium characteristics defined as follows:

$$\kappa_l=\frac{\omega}{\nu_l}+ia_l\omega^2,\quad \kappa_d=\frac{\omega}{\nu_d}+ia_d\omega^2,\quad \kappa_s=\frac{\omega}{\nu_s}+ia_s\omega^2, \tag{2}$$

and $k_x^{\rm inc}$ is the wave-vector component of the incident wave projected on the virtual average surface ($z=0$). For inhomogeneous waves ($\beta_{\rm inc}\neq 0$), this quantity is defined in general[7–9] as

$$k_x^{\rm inc}=k_{\rm inc}\sin\theta_{\rm inc}+i\alpha_{\rm inc}\sin\theta_{\rm inc}-i\beta_{\rm inc}\cos\theta_{\rm inc}, \tag{3}$$

where $\theta_{\rm inc}$ is the angle of incidence and $k_{\rm inc}$, $\alpha_{\rm inc}$, and $\beta_{\rm inc}$, are the 3 specific characteristics (wave number, attenuation, and heterogeneity) of the incident wave satisfying the complex valued dispersion relation:

$$k_{\rm inc}^2-\alpha_{\rm inc}^2-\beta_{\rm inc}^2=\mathrm{Re}(\kappa_l)^2-\mathrm{Im}(\kappa_l)^2,\qquad k_{\rm inc}\cdot\alpha_{\rm inc}=\mathrm{Re}(\kappa_l)\cdot\mathrm{Im}(\kappa_l). \tag{4}$$

Consequently, the z component $K_{\rm inc}$ can be expressed as

$$K_{\rm inc}=k_{\rm inc}\cos\theta_{\rm inc}+i\alpha_{\rm inc}\cos\theta_{\rm inc}+i\beta_{\rm inc}\sin\theta_{\rm inc} \tag{5}$$

(in the case of normally incident inhomogeneous waves, we simply have that $k_x^{\rm inc}=-i\beta_{\rm inc}$ and $K_{\rm inc}=k_{\rm inc}+i\alpha_{\rm inc}$). Also in Eq. (1), k_m is the wave-vector component of the mth-order scattered wave projected on the surface which obeys the generalized Snell laws for periodic gratings, i.e.,

$$k_m=k_x^{\rm inc}+\mathrm{m}(2\pi/\Lambda)\quad \text{for all integer values of } m. \tag{6}$$

This component is identical for reflected, transmitted, and in-plate generated waves within each order.

Further, the following familiar definitions were used defining the magnitude of the z components of the scattered waves in the mth order:

$$K_{rm}^2=\kappa_l^2-k_m^2,\quad K_{tm}^2=\kappa_l^2-k_m^2,\qquad K_{dm}^2=\kappa_d^2-k_m^2,\quad K_{sm}^2=\kappa_s^2-k_m^2. \tag{7}$$

Finally, we define

$$I_{0n}=\frac{1}{K_{\rm inc}}\int_0^\Lambda \exp[i\{K_{\rm inc}F(x)-2\pi nx/\Lambda\}]dx,$$

$$I_{mn}^{p\pm}=\frac{\pm 1}{K_{pm}}\int_0^\Lambda \exp[i\{\pm K_{pm}F(x)+2\pi(m-n)x/\Lambda\}]dx,$$

for $p=r,d,s$, and m,n integers (8a)

$$J_{mn}^{p\pm}=\int_0^\Lambda \exp[i\{\pm K_{pm}d+2\pi(m-n)x/\Lambda\}]dx,$$

for $p=d,s,t$, and m,n integers. (8b)

The linear system represented by Eq. (1) is in fact an infinite system of coupled linear equations, however, in order to implement it numerically one is obliged to truncate it to a finite order M, neglecting all reflected, transmitted, and in-plate scattered orders with indices in absolute value of $M+1$ or larger. In all of the illustrations shown in this paper an

approximation to order 4 was found to be sufficient based on the criterion that the inclusion of the fifth order in the calculations did not affect the reflection coefficients of order -4 through 4 by more than 2 dB.

This system is valid for homogeneous waves as well as for inhomogeneous waves with complex wave numbers. The characteristics of the generated waves [i.e., the scattering angle (measured from the positive z-axis counterclockwise), heterogeneity coefficient, and positive-valued wave number and attenuation parameters] can be obtained from a combination of the complex-valued grating equation [Eq. (6)] and the dispersion equation [Eq. (7)]. For instance for the in-plate dilatational wave of order m, θ_{dm}, β_{dm}, k_{dm}, and α_{dm} can be calculated by representing the x and z components (k_m and K_{dm}) by

$$k_{dm}\sin\theta_{dm}+i\alpha_{dm}\sin\theta_{dm}-i\beta_{dm}\cos\theta_{dm}$$

and

$$k_{dm}\cos\theta_{dm}+i\alpha_{dm}\cos\theta_{dm}+i\beta_{dm}\sin\theta_{dm},$$

respectively, which translates Eqs. (6) and (7) to

$$\begin{aligned} &k_{dm}\sin\theta_{dm}=k_{\mathrm{inc}}\sin\theta_{\mathrm{inc}}+m(2\pi/\Lambda),\\ &\alpha_{dm}\sin\theta_{dm}-\beta_{dm}\cos\theta_{dm}=\alpha_{\mathrm{inc}}\sin\theta_{\mathrm{inc}}\\ &\qquad\qquad -\beta_{\mathrm{inc}}\cos\theta_{\mathrm{inc}}, \end{aligned} \tag{9}$$

$$\begin{aligned} &k_{dm}^2-\alpha_{dm}^2-\beta_{dm}^2=\mathrm{Re}(\kappa_d)^2-\mathrm{Im}(\kappa_d)^2,\\ &k_{dm}\cdot\alpha_{dm}=\mathrm{Re}(\kappa_d)\cdot\mathrm{Im}(\kappa_d). \end{aligned} \tag{10}$$

Similar systems of equations have to be solved to get the characteristics of the reflected, transmitted, and in-plate shear waves. Particular attention has to be paid to the sign of the z-axis projection of the wave numbers. The magnitude of these z projections is defined by Eq. (7), their sign remains ambiguous. In the case of plane homogeneous waves we determine the sign of all scattered waves in the different orders by the Sommerfeld conditions, saying that no scattered waves can be generated with exponentially growing amplitude away from an interface. The Sommerfeld conditions do not hold any more when we are dealing with incident bulk inhomogeneous waves. As we know, the scattered waves in reflection and transmission can be bulk inhomogeneous waves as well. In reflection and transmission we require that K_{rm} and K_{tm} have the appropriate sign so that they represent waves that are propagating away from the outside surfaces of the plate, i.e., $\mathrm{Re}(K_{rm})\leqslant 0$ and $\mathrm{Re}(K_{tm})\geqslant 0$. Further, we determine the sign of K_{dm} and K_{sm} as follows:

Define dilatational ($p=d$) and shear ($p=s$) critical angles as follows:

$$\theta_p^{\mathrm{cr}}=\mathrm{Arcsin}(\nu_l/\nu_p).$$

If $[180-\theta_p^{\mathrm{cr}}>\theta_{rm}\,\mathrm{and}\,\beta_{rm}>0]$ or $[180+\theta_p^{\mathrm{cr}}<\theta_{rm}$ and $\beta_{rm}<0]$ then $\mathrm{Sign}(\mathrm{Re}(K_{pm}))$ equals -1;

or equivalently $K_{pm}:=-|\mathrm{Re}(K_{pm})|-i\,\mathrm{Sign}(\mathrm{Re}(K_{pm}))\cdot\mathrm{Im}(K_{pm})$.

In all other cases $\mathrm{Sign}(\mathrm{Re}(K_{pm}))$ should be 1.

These conditions correspond to a generalized version of the criteria reported by Deschamps[9] in his theoretical and experimental study of the reflection (and transmission) of a bulk inhomogeneous wave incident on a liquid–solid and liquid–solid–liquid system with plane interfaces. He showed that special attention needs to be given to the twofold solution of the generalized Snell laws in order to match the experimental data to the theoretical prediction.

In Fig. 5(a) we show the reflection coefficient R_0 (specular reflection) as a function of frequency in the case of a homogeneous plane wave at normal incidence. The scattered orders in reflection [$R_{\pm 1}$, $R_{\pm 2}$, $R_{\pm 3}$, and $R_{\pm 4}$ (all in dB)] are depicted in Fig. 5(b). In the frequency interval ranging from 0.5 to 3 MHz we observe quite a number of ''anomalies'' in the reflection coefficient, as well in the specular reflection direction as in the scattered orders. The position of the different features at various frequencies can be explained by taking a close look at Fig. 6. First of all, two major dips occur in R_0 at 1.21 and 2.42 MHz. These anomalies correspond to the ''limiting'' frequencies of the longitudinal resonances S_2 and A_3 at normal incidence for a smooth 2-mm-thick brass plate (indicated on top of Fig. 6 by the italicized-underlined numbers: 1.210 and 2.420 MHz). Since the height of the corrugation is taken to be much smaller than the plate thickness, we are still able to observe these so-called cutoff modes. All other ''limiting'' frequencies (nonitalicized-underlined numbers on top of Fig. 6) correspond to shear

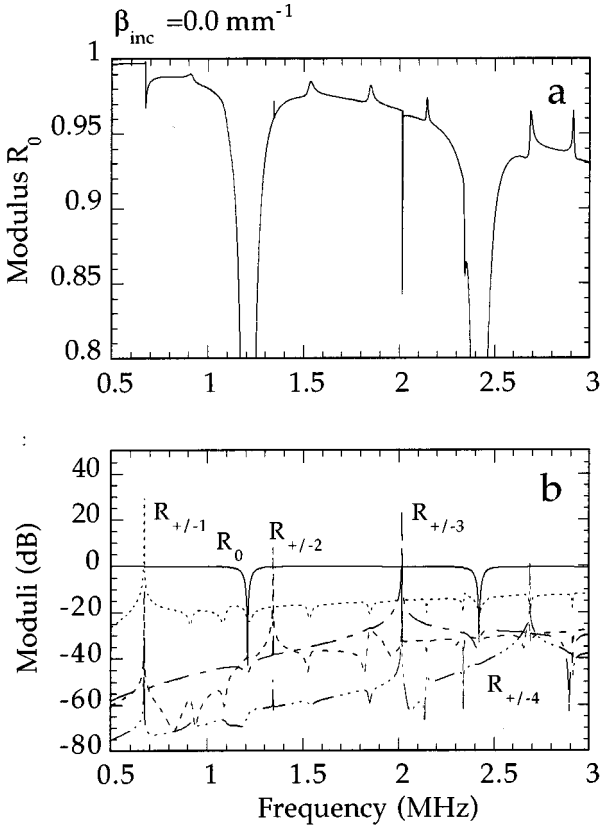

FIG. 5. (a) R_0 modulus for a homogeneous wave normally incident on a sawtooth corrugated brass plate in water ($d=2$ mm, $\Lambda=2.2$ mm, $h=50$ μm). (b) Moduli of the diffracted orders in reflection for a homogeneous wave (in dB) [same plate parameters as in (a)].

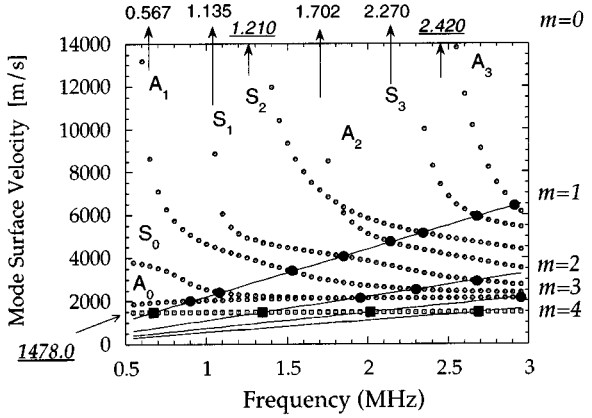

FIG. 6. Mode identification figure at normal incidence for a 2-mm-thick brass plate with periodical corrugated surface ($\Lambda=2.2$ mm).

resonances at normal incidence and cannot be generated by a pure longitudinal incident plane wave at $\theta=0°$ because the in-plate displacement in this case is also strictly in the z direction. A second group of features corresponds to frequencies at the intersection points of the dispersion curves for a smooth brass plate of 2 mm with the lines

$$\nu = f\Lambda/m, \quad \text{for } m = 1,2,3,4,\ldots, \tag{11}$$

in which ν denotes the velocity along the water/brass surface, f is the frequency, and Λ is the corrugation periodicity. The cuttoff frequencies (representing the first group of features) correspond to the special case for which $m=0$. At every frequency corresponding to an intersection of these lines with the dispersion curves, an anomaly is observed. A last group corresponds to the intersection points of the horizontal line at the Stoneley velocity (1478.0 m/s) and the above-mentioned straight lines for different (nonzero) integer values of m. Classically, all these frequency positions for which anomalies occur in the reflection coefficients, are interpreted as ''critical'' frequencies for which a homogeneous wave can stimulate a specific eigenmode of the system. This is only partly true however. We note that the only features for which we observe sharp peaks (larger than 0 dB) in the coefficients R_m for each value of m, occur at frequencies corresponding to intersections of the straight lines with the horizontal line at the Stoneley velocity, i.e., exactly at every multiple of 0.6718 MHz. These are indeed the only conditions in which a homogeneous wave can generate and stimulate a surface wave, in this case a Stoneley wave. Depending on the value of m at the interaction point the Stoneley wave shows up as the diffracted wave of that specific order, but in all cases it has the same characteristic exponential decay (after normalizing by frequency). Since R_m equals R_{-m} for homogeneous waves, Stoneley waves are created in both directions along the surface.

We emphasize once more that no other plate mode is generated nor stimulated by an incident homogeneous wave at normal incidence. The scattered orders in reflection and transmission corresponding to propagating waves away from the upper and lower surfaces are all homogeneous waves and as a consequence they cannot satisfy the properties of the leaking field typical for a particular Lamb mode of the system.

Just like in the case of plane interfaces, we have to consider the scattering of the more general complex harmonic wave to accurately describe plate-mode stimulation for corrugated layers at normal incidence. Each feature observed in the reflection coefficient of homogeneous waves can get arbitrarily large by insonifying the plate at normal incidence with an inhomogeneous wave with the appropriate value for the heterogeneity β_{inc}. Figures 7–12 illustrate this for three of the predicted anomalies.

In Fig. 7 we show the reflection moduli for an incident inhomogeneous wave with exponential decay $\beta_{\text{inc}}=0.061065$ mm^{-1}. At this heterogeneity value, the R_{-1} reflection coefficient [along with the T_{-1} transmission coefficient (not shown)] exhibits a well pronounced maximum at $f=1.53053$ MHz. This means that these parameter conditions are favorable for the generation and stimulation of the A_1-plate mode in the -1st diffraction order. The -1st-order scattered wave reflects at an angle of 206.073° (measured counterclockwise from the positive z axis) and has an exponential decay of -0.06796 mm^{-1}. These are exactly the characteristics of the first asymmetric eigenmode in a smooth brass plate at 1.53053 MHz. Moreover, the surface wave velocity and displacement vector inside the corrugated plate agrees with the velocity and displacement calculations for the A_1 mode in a plane-parallel 2-mm brass plate at that frequency. Figure 8

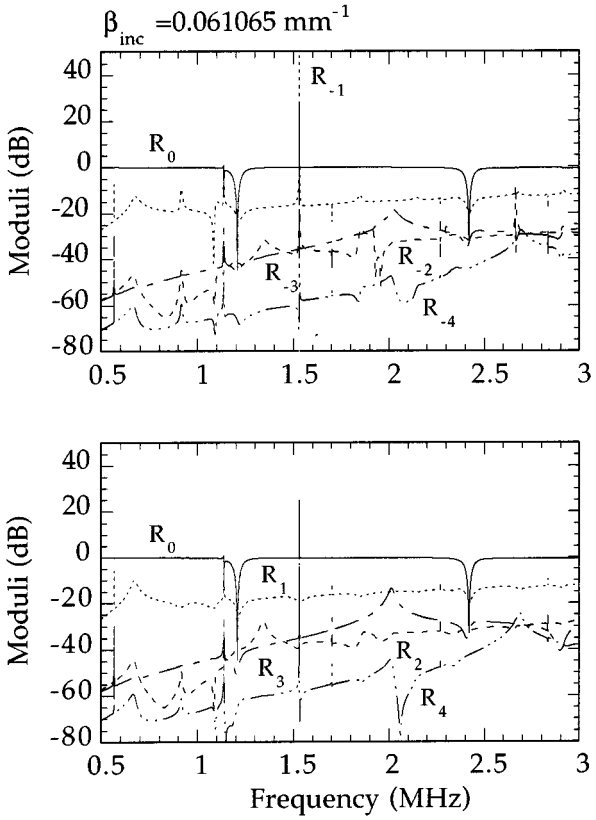

FIG. 7. Moduli of the diffracted orders in reflection for the A_1 mode stimulating inhomogeneous wave ($\beta_{\text{inc}}=0.061065$ mm^{-1}) in -1st diffraction order at 1.53 MHz. [Same plate parameters as in Fig. 5(a).]

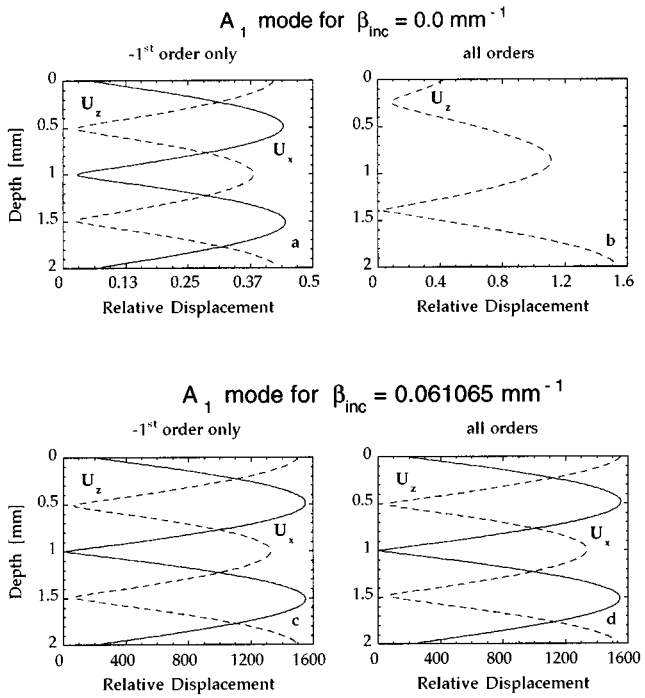

FIG. 8. Relative displacement components inside the 2-mm rough brass plate at 1.53 MHz. (a) Calculation for an incident homogeneous wave using −1st diffraction order only. (b) Calculation for an incident homogeneous wave using interference of all orders. (c) Calculation for the mode stimulating inhomogeneous wave using −1st diffraction order only. (d) Calculation for the mode stimulating inhomogeneous wave using interference of all orders.

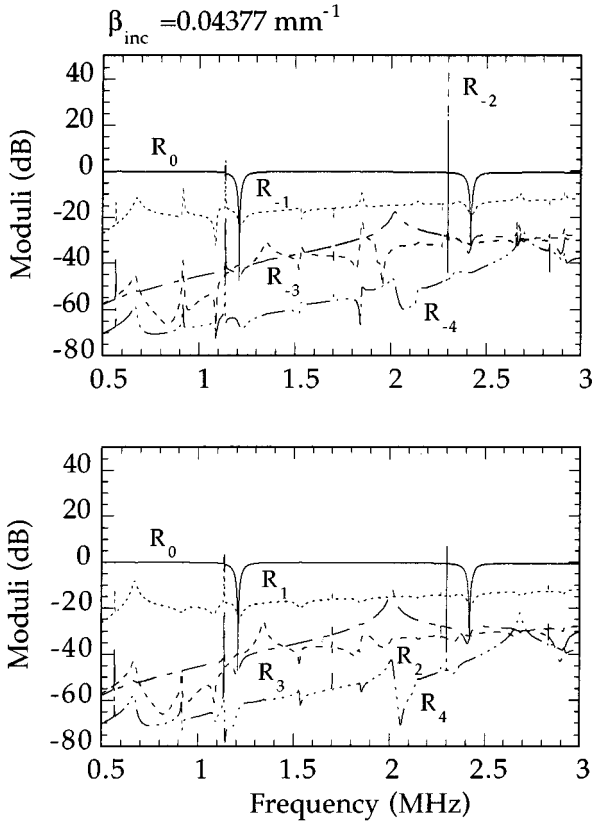

FIG. 9. Moduli of the diffracted orders in reflection for the A_1 mode stimulating inhomogeneous wave ($\beta_{\text{inc}}=0.04377\ \text{mm}^{-1}$) in −2nd diffraction order at 2.3 MHz. [Same plate parameters as in Fig. 5(a).]

compares the in-plate displacements for the homogeneous and specific inhomogeneous wave at 1.53053 MHz. All displacements shown are calculated relative to the displacement of the incident wave at the (virtual) position ''$x=0$, $z=0$.'' In the first column [Fig. 8(a) and (c)] we plotted the relative displacements calculated for the −1st diffraction order only. The second column [Fig. 8(b) and (d)] illustrates the total in-plate relative displacement, calculated from the interference of all (negative and positive) orders. Four observations can be made: (1) the A_1 asymmetrical vibration mode is highly stimulated by the incident inhomogeneous wave, orders of magnitude larger than in the case of a homogeneous plane wave; (2) (as indicated above) the homogeneous plane wave only accounts for a global z displacement inside the plate (no net shear displacement), which is quite different from the displacement in one separate diffraction order; (3) the in-plate displacement calculated for the specific mode stimulating complex harmonic wave over all diffraction orders is not much different from the displacement in the −1st order only, indicating that all of the energy is concentrated in that scattering order (the interference with other orders is negligible); and (4) since only small and gradual corrugations are taken into account (Rayleigh assumption), the displacement fields at resonance conditions show either symmetrical or asymmetrical behavior even though the layer interfaces are not similar. Clearly this will not be the case when steep gradients occur in the profile and ''standing'' waves have to be taken in consideration between profile elevations.

Since no previous treatments of plane inhomogeneous wave scattering and mode stimulations are known to us, we include two other examples to demonstrate these four observations. Figures 9 and 10 illustrate the stimulation of the A_1 asymmetrical vibration mode in −2nd diffraction order for $\beta_{\text{inc}}=0.04377\ \text{mm}^{-1}$ at a frequency of 2.300 MHz. The incident complex harmonic wave again induces a much higher excitation level compared to the homogeneous wave. Note for instance the large reflection coefficient R_{-2}, and the huge relative in-plate displacements with all the energy confined in the −2nd diffraction direction. Figures 11 and 12 finally, visualizes the results for the S_0 stimulation in the −1st diffraction order at 1.09374 MHz by an inhomogeneous wave with heterogeneity parameter $0.09454\ \text{mm}^{-1}$.

To conclude this section, three additional remarks are in order: (1) Due to symmetry properties at normal incidence, the same eigenmode can be stimulated in positive x direction (extrema for R_{+m} and T_{+m}) by changing the heterogeneity of the incident complex harmonic wave from $+\beta_{\text{inc}}$ to $-\beta_{\text{inc}}$. (2) The use of incident inhomogeneous waves can lead to additional material information since their reflection coefficients show the extra features which are related to the ''limiting'' frequencies for shear resonances at normal incidence. These features appear at the intersection points of the brass plate dispersion curves and $\nu=\textit{infinity}$ (corresponding to $m=0$). (3) If a system consists of several layers separated by corrugated interfaces with different periodicities, it is the least common multiple of all periodicities involved that con-

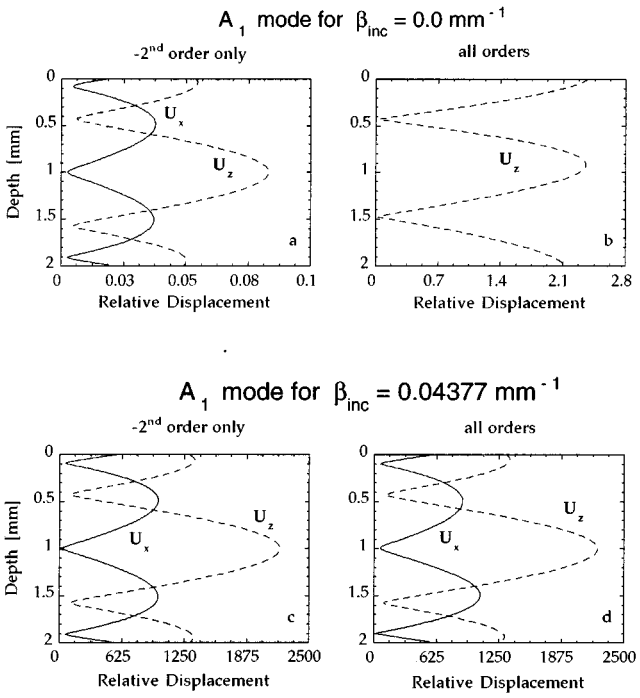

FIG. 10. Relative displacement components inside the 2-mm rough brass plate at 2.3 MHz. (a) Calculation for an incident homogeneous wave using −2nd diffraction order only. (b) Calculation for an incident homogeneous wave using interference of all orders. (c) Calculation for the mode stimulating inhomogeneous wave using −2nd diffraction order only. (d) Calculation for the mode stimulating inhomogeneous wave using interference of all orders.

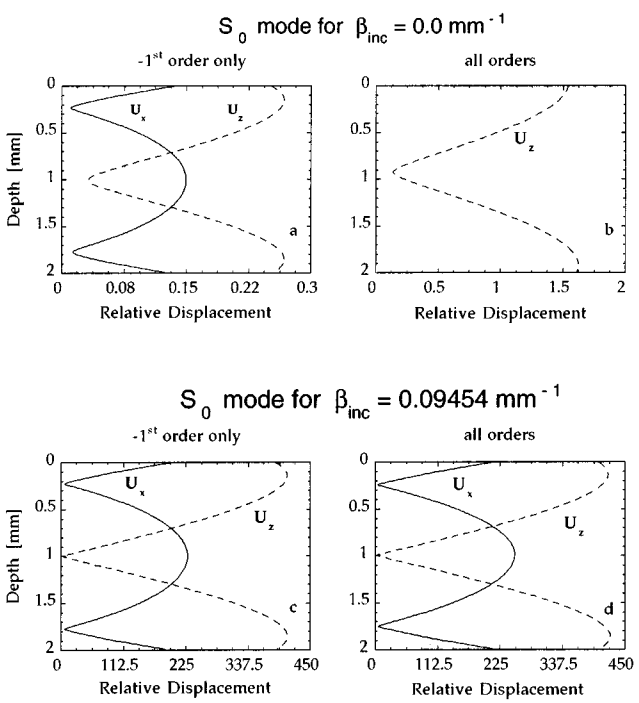

FIG. 12. Relative displacement components inside the 2-mm rough brass plate at 1.094 MHz. (a) Calculation for an incident homogeneous wave using −1st diffraction order only. (b) Calculation for an incident homogeneous wave using interference of all orders. (c) Calculation for the mode stimulating inhomogeneous wave using −1st diffraction order only. (d) Calculation for the mode stimulating inhomogeneous wave using interference of all orders.

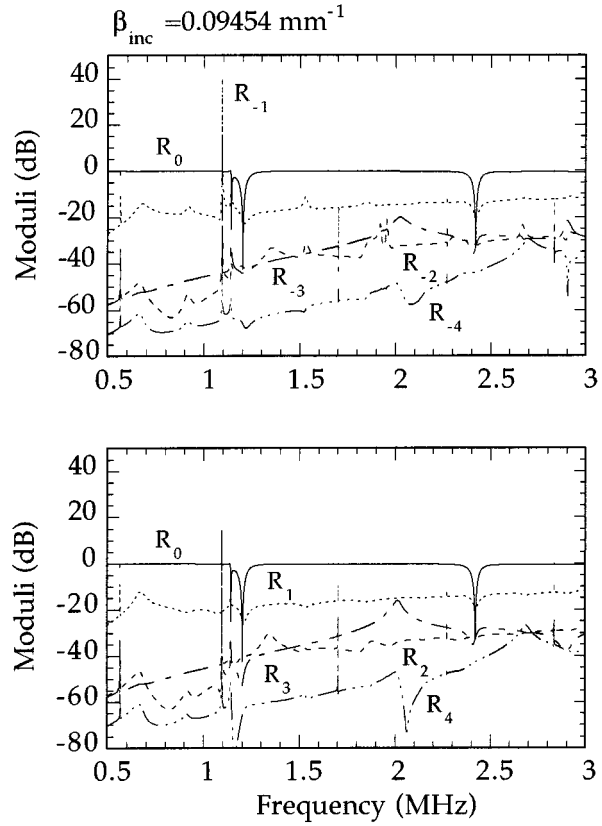

FIG. 11. Moduli of the diffracted orders in reflection for the S_0 mode stimulating inhomogeneous wave (β_{inc}=0.09454 mm^{-1}) in −1st diffraction order at 1.094 MHz. [Same plate parameters as in Fig. 5(a).]

trols the diffraction of a plane wave. In the case of two different periodicities Λ_1 and Λ_2 with a least common multiple Λ (and assuming that Λ_1 and Λ_2 are not integer multiples of each other), the number of ''anomaly'' positions in a fixed frequency range is greatly multiplied when compared to a case for which the governing periodicity would be either Λ_1 or Λ_2. Consequently, in the numerical implementation, the dimension of the transfer matrix deduced from the linear system in Eq. (1) increases significantly because more orders need to be taken into account.

II. SCATTERING FROM A LIQUID–SOLID HALF-SPACE WITH PERIODICALLY CORRUGATED SURFACE

In this section we apply the complex harmonic wave scattering theory at periodic rough surfaces in the case of a single corrugated boundary between a liquid and a solid half-space. We will demonstrate that Stoneley and Rayleigh waves can be stimulated at normal incidence by homogeneous and inhomogeneous waves with a proper choice of the heterogeneity parameter.

A. Water–brass half-space

The Stoneley velocity for a water–brass system with a plane interface boundary equals 1478.0 m/s, whereas the Rayleigh velocity is 2128.46 m/s. The absolute value of the heterogeneity characteristic for the exponential decaying parts of these surface waves in water at a frequency of 1

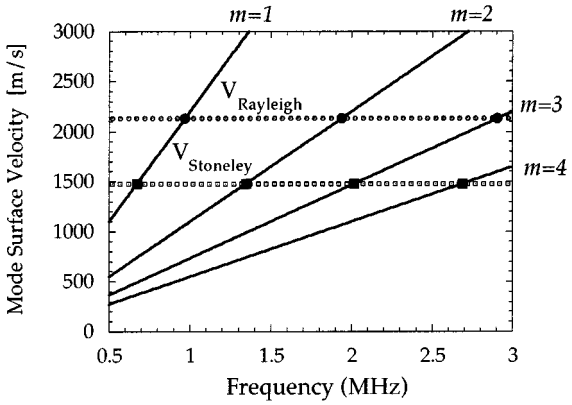

FIG. 13. Mode identification figure at normal incidence for a water–brass system with periodical corrugated interface ($\Lambda=2.2$ mm).

MHz is 0.0937 and 0.0634 mm^{-1}, respectively. The liquid component of the Stoneley wave travels exactly parallel to the surface. The Rayleigh wave is leaky and radiates in a direction equal to the Rayleigh angle: 44.048°.

Given this information, Fig. 13 shows the possible critical frequencies for Stoneley and Rayleigh wave stimulation at a liquid–brass interface with a 2.2-mm periodic corrugation. We predict that in the frequency range of 0.5 to 3 MHz it is possible to obtain a Stoneley wave stimulation at four different frequencies, each time in a different diffraction order. Indeed, Fig. 14 clearly shows four major anomalies in the reflection moduli for an incident homogeneous plane wave at normal incidence, occurring at multiple values of 0.6718 MHz. Successive anomalies correspond to extrema in successively higher-order reflection coefficients and indicate that the Stoneley wave is stimulated in consecutively higher scattered orders. Solving the generalized Snell relations, one can easily verify that the propagation direction of the scattered waves in these orders is parallel to the interface, that the velocity equals 1478.0 m/s and that the exponentially decaying component corresponds exactly to the characteristic Stoneley wave decay (when normalized by the frequency).

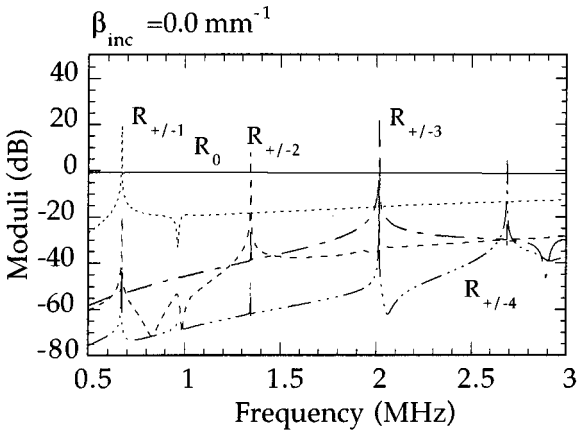

FIG. 14. Moduli of the diffracted orders in reflection for an incident homogeneous wave at a sawtooth corrugated water–brass interface ($\Lambda=2.2$ mm $h=50$ μm). Peaks are corresponding to Stoneley-mode stimulation.

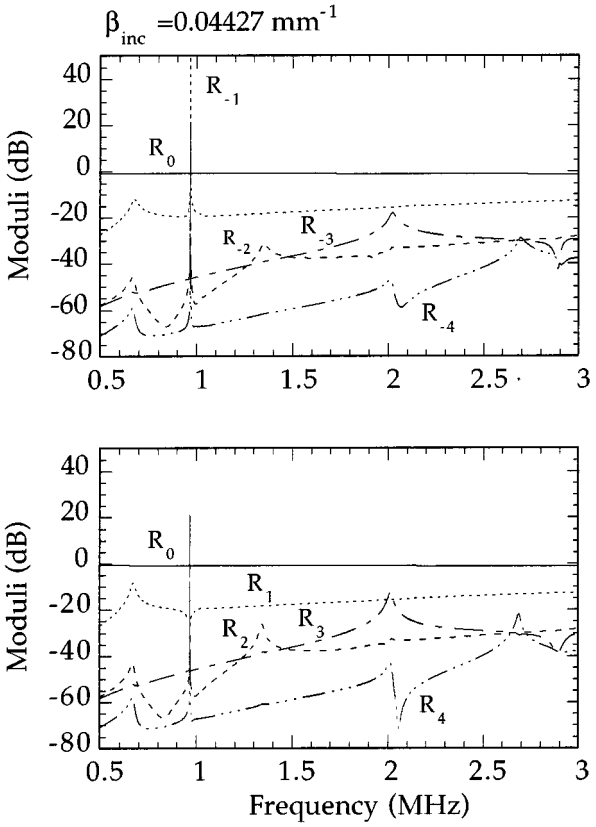

FIG. 15. Moduli of the diffracted orders in reflection for the Rayleigh wave stimulating inhomogeneous wave ($\beta_{inc}=0.04427$ mm^{-1}) in -1st diffraction order at 0.9674 MHz on a corrugated water–brass interface. (Same interface parameters as in Fig. 13.)

Looking again at Fig. 13, we also find three critical frequencies for which Rayleigh wave stimulation may occur: in first, second, and third order (plus and minus). In Fig. 15, we show the stimulation of the -1st-order diffracted Rayleigh wave by a complex harmonic wave with heterogeneity coefficient $\beta_{inc}=0.04427$ mm^{-1}. R_{-1} clearly shows a maximum at 0.9674 MHz. The generalized Snell relations yield a heterogeneity parameter $\beta_{r-1}=-0.06159$ mm^{-1} (at 0.9674 MHz) and a direction 44.053° for the scattered inhomogeneous wave in the -1st diffraction order, which agrees with the information obtained from the plane boundary calculations. Because of the excellent agreement of the fundamental characteristics we may conclude that the wave stimulated in -1st order is really the Rayleigh wave.

B. Water–steel half-space

For a water–steel system (steel parameters: dilatational velocity: $\nu_d=5790$ m/s; dilatational attenuation: $a_d\omega^2=4\times10^{-6}$ Np/mm at 1 MHz; shear velocity: $\nu_s=3200$ m/s; shear attenuation: $a_s\omega^2=2\times10^{-5}$ Np/mm at 1 MHz; density: 7900 kg/mm^3) with a plane interface boundary the Stoneley velocity equals 1479.59 m/s, whereas the Rayleigh velocity is 2959.25 m/s. It is remarkable that the Rayleigh velocity is approximately twice the value of the Stoneley velocity. Curiously enough this means that the first (second, etc....)-order diffracted Rayleigh wave occurs at the same

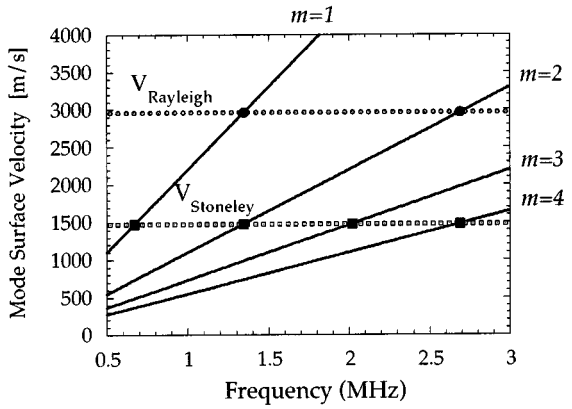

FIG. 16. Mode identification figure at normal incidence for a water–stainless steel system with periodical corrugated interface ($\Lambda=2.2$ mm).

frequency as the second (fourth, etc....)-order diffracted Stoneley wave (see Fig. 16). In Figs. 17 and 18 we evaluated the region around 1.345 MHz and found indeed that a homogeneous wave can stimulate a Stoneley wave in the second diffracted order at the same frequency for which an inhomogeneous wave with $\beta_{\text{inc}}=0.03082$ mm^{-1} stimulates the minus-first-order diffracted Rayleigh wave. This particular inhomogeneous wave really stimulates the leaky Rayleigh wave, even though it may seem as if other diffraction orders somehow interfere because of their large reflection coefficients. To prove this, we plotted in Fig. 19 the resulting relative displacements in the steel half-space for the -1st-order component only and for the total interference of all orders. It is clear that approximately all of the energy propagates in the -1st-order direction, and that the x and z components correspond to the commonly known Rayleigh-type displacements.

III. STUDY OF SOME CORRUGATION PARAMETERS AND PLATE THICKNESS

A. Corrugation profile: Sawtooth versus sine profiles

Figure 20 compares the theoretical calculations for a water–brass–water system having a plane lower interface

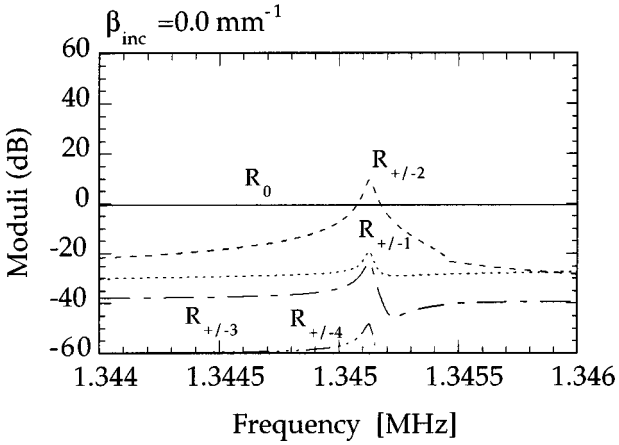

FIG. 17. Moduli of the diffracted orders in reflection for an incident homogeneous wave at a sawtooth corrugated water-stainless steel interface ($\Lambda=2.2$ mm, $h=50$ μm) as a function of frequency, in the neighborhood of the $\pm$2nd order Stoneley mode frequency.

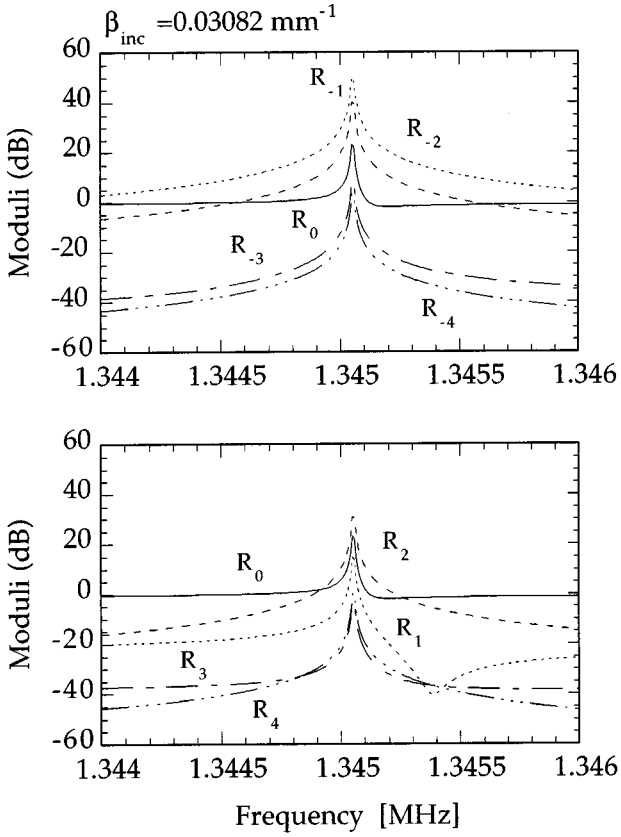

FIG. 18. Moduli of the diffracted orders in reflection for the -1st diffraction order Rayleigh wave stimulating inhomogeneous wave ($\beta_{\text{inc}}=0.03082$ mm^{-1}) at a sawtooth corrugated water–stainless steel interface ($\Lambda=2.2$ mm, $h=50$ μm) in the same frequency range as used in Fig. 17.

and an upper interface corrugated by a sawtooth-shaped profile (open circles) with the results for a sine shaped corrugation (closed circles) for the same periodicity (2.2 mm) and height (150 μm). One observes no major difference for 0, ±1, and ±2. On the other hand there seems to be quite a difference for higher diffraction orders. Actually, it is not yet clear why the difference appears only in the higher orders.

Sine and sawtooth corrugated profiles lead to easy closed analytical evaluations for the integrals [Eq. (8)] in-

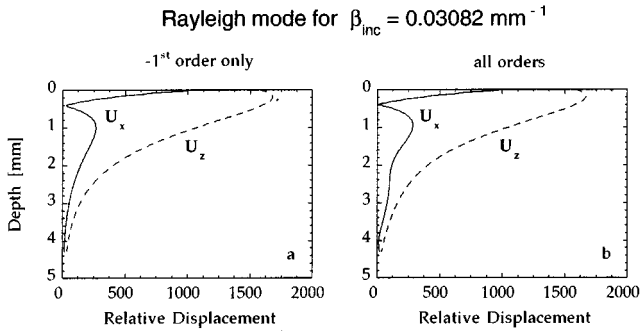

FIG. 19. Relative Rayleigh mode displacement components inside the stainless-steel half-space at 1.345 MHz. (a) Calculation for the Rayleigh mode stimulating inhomogeneous wave using -1st diffraction order only. (b) Calculation for the Rayleigh mode stimulating inhomogeneous wave using interference of all orders.

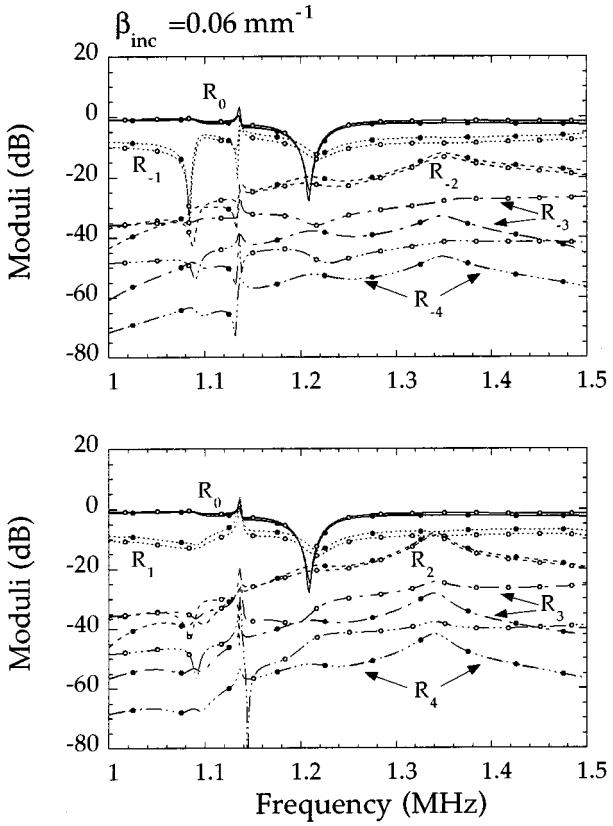

FIG. 20. Comparison between the moduli of the diffracted orders in reflection for a sawtooth (open circles) and sinusoidal (filled circles) corrugated brass plate for an inhomogeneous plane wave ($\beta_{\text{inc}}=0.06\ \text{mm}^{-1}$) at normal incidence ($d=2$ mm, $\Lambda=2.2$ mm, $h=150\ \mu$m).

volved in constructing the transfer matrix. More complicated corrugations of arbitrary profile $F(x)$ can be analyzed either by a single FFT evaluation or by use of their Fourier series expansion. For instance, the second integral in Eq. (8a) can be evaluated as follows using:

$$I_{mn}^{p}=\frac{1}{K_{pm}}\int_0^{\Lambda}\exp[i\{K_{pm}F(x)+2\pi(m-n)x/\Lambda\}]dx$$
$$=\frac{\Lambda}{K_{pm}}\sum_{r_2=-\infty}^{+\infty}\cdots\sum_{r_N=-\infty}^{+\infty}J_{r_1}\left(\frac{K_{pm}h}{2}A_1\right)$$
$$\cdot J_{r_2}\left(\frac{K_{pm}h}{2}A_2\right)\cdots J_{r_n}\left(\frac{K_{pm}h}{2}A_N\right)$$
$$\times\exp[i(r_1\varphi_1+r_2\varphi_2+\cdots+r_N\varphi_N)], \tag{12}$$

with

$$F(x)=\frac{h}{2}\sum_{j=1}^{n}A_j\sin\left(\frac{2\pi}{\Lambda}jx+\varphi_j\right)$$

and

$$r_1=m-n-2r_2-3r_3-\cdots-Nr_N.$$

In view of preceding analysis it is obvious that sawtooth and sine profiles yield quite similar results. The first term in the Fourier expansion of a sawtooth profile is essentially equal to the sine corrugation considered in the comparison. The other terms in the Fourier series, all with periods that are odd fractions of the repetition period, are less important and their contribution is only significant at the levels of the third and fourth diffraction orders.

Apart from the shape of the corrugation, there are several other physical parameters that can change independently during a production process and need to be controlled by NDE measurements. In what follows, we investigate the influence of small deviations in plate thickness, corrugation periodicity, and corrugation height on the ideal stimulation characteristics (at normal incidence: frequency and heterogeneity parameter) of the A_1-Lamb mode in -1st diffraction order. In addition, Figs. 21–23 contain complementary information about the shift of the -1st diffraction order emission angle of this particular Lamb mode, which is a tractable and easy measurable quantity.

B. Plate thickness 1.5 mm$\leqslant d\leqslant$3.0 mm ($\Lambda=2.2$ mm; $h=50\ \mu$m)

The plate thickness is certainly one of the most sensitive parameters. In Fig. 21, we observe that the frequency of the A_1-Lamb mode diminishes monotonically from 1.75 MHz at 1.5 mm to 1.26 MHz at 3.0-mm thickness. The dashed line connecting the squares represent the thickness dependence of the emission angle in the -1st diffraction order at ideal stimulation conditions. Again we observe a monotonic behavior, a result that could be readily predicted from the dispersion curves of plane parallel plates. The heterogeneity coefficient β_{inc} of the incident complex harmonic wave for which A_1-mode stimulation occurs (full line connected open circles), also extends over a wide range, but does not show a monotonic behavior. A simple calculation of the heterogeneity parameter of the -1st scattered component in reflection [based on Eq. (9) for normal incidence] tells us that the leaking field of the A_1 mode will show the largest exponential decay across the wavefront for thicknesses between 1.9 and

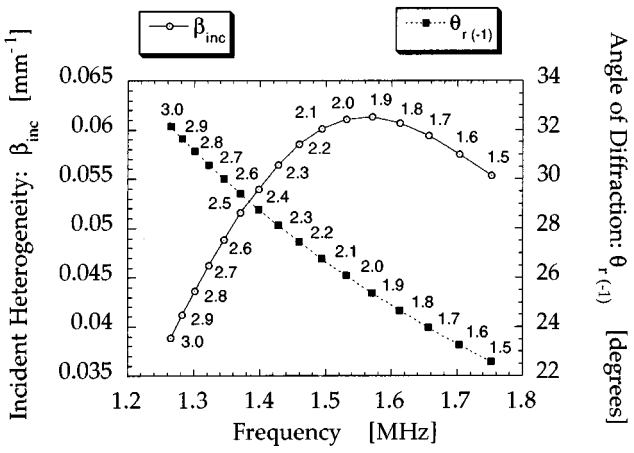

FIG. 21. Critical (f, β_{inc}) positions (full line connected circles) for the stimulation of the A_1 Lamb mode in the -1st diffraction order at normal incidence as a function of the plate thickness (1.5 mm$\leqslant d\leqslant$3.0 mm) in the case of a brass plate with a sawtooth corrugated upper surface ($\Lambda=2.2$ mm, $h=50\ \mu$m). The dashed line connected filled squares illustrate the change in emission angle (-1st-order diffraction angle) due to the variation in plate thickness.

2.0 mm. In other words, when applied to an experimental situation, the leaking field in the -1st diffraction order will be best localized in this range (the A_1-mode radiates only over a small distance).

It is obvious that plate thickness variations (even over much smaller intervals than shown here) can be responsible for dissatisfying a certain known ''resonance'' condition used as a prescribed standard norm in a manufacturing process. Any small deviation from the ideal mode stimulation requirements shows up immediately as a loss of leaking energy in the postulated diffraction order and as a change in emission angle.

C. Corrugation periodicity 1.5 mm$\leqslant\Lambda\leqslant$2.5 mm ($h$=50 μm; d=2.0 mm)

Analogous conclusions can be drawn when investigating the influence of the periodicity Λ of the corrugation. For a fixed plate thickness and corresponding dispersion curves, the variation in Λ clearly affects the frequency and emission angle of the stimulated plate mode. For instance, the intersection point of the A_1-mode dispersion curve with the line $\nu=f\cdot\Lambda$ [Eq. (11) for $m=1$] moves up or down in frequency for smaller or larger values of periodicity, respectively. At the same time, the angle of emission increases (respectively decreases). Just like in the study of plate thickness influence, the heterogeneity coefficient β_{inc} of the ideal incident complex harmonic wave for A_1 mode stimulation does not show a monotonic behavior as a function of periodicity (Fig. 22). The maximum again corresponds to the condition for which the A_1 mode is best localized. The fact that the maximum again occurs exactly at a value of 1.9 mm (this time for Λ) is only a coincidence.

The behavior of the essential mode-characterization parameters (frequency, incident heterogeneity, and emission angle) on plate thickness and corrugation periodicity is quite similar. This is related to their cognate influence on the position of the intersection points in a mode determination figure like Fig. 6. Simply put, plate thickness variations lead to compression or expansion of the dispersion curves in the same frequency interval while periodicity affects the slope of the intersection lines. Since the influence is not linear in d or Λ, one should be able to determine the relative importance of those parameters in the deviation from a standard norm by making ample observations.

Finally, in the following section, we investigate the influence of another important grating parameter: the height of the corrugation.

D. Corrugation height 25 μm$\leqslant h\leqslant$300 μm (d=2.0 mm; Λ=2.2 mm)

As can be seen from Fig. 23, the variation of the frequency-heterogeneity requirement for ideal mode stimulation as a function of the corrugation height is not all that impressive. Over a range of about 300 μm, the frequency shift amounts to only 7–8 kHz while the incident heterogeneity coefficient changes only by about 8%.

Unlike plate thickness and corrugation periodicity, the influence of the height of the corrugation does not appear to be a large effect (at least not within the limitations of the Rayleigh assumption). This means that very sensitive equipment will be needed to capture changes due to height deviations of the corrugation. The same conclusion holds for slight profile alterations. The situation becomes even far more complicated when all sample parameters deviate from their standards at the same time during a manufacturing process. Finding out and deciding which corrections are to be made can be a laborious task.

E. Independence relations

Assuming that attenuation is small or proportional to frequency, one can verify the following theoretical indepen-

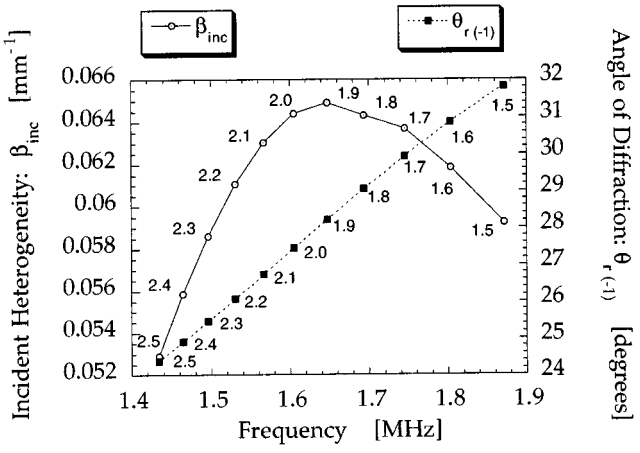

FIG. 22. Critical (f, β_{inc}) positions (full line connected circles) for the stimulation of the A_1 Lamb mode in the -1st diffraction order at normal incidence as a function of the corrugation periodicity (1.5 mm$\leqslant\Lambda\leqslant$2.5 mm) in the case of a brass plate with a sawtooth corrugated upper surface (h=50 μm, d=2.0 mm). The dashed line connected filled squares illustrate the change in emission angle (-1st-order diffraction angle) due to the variation in corrugation periodicity.

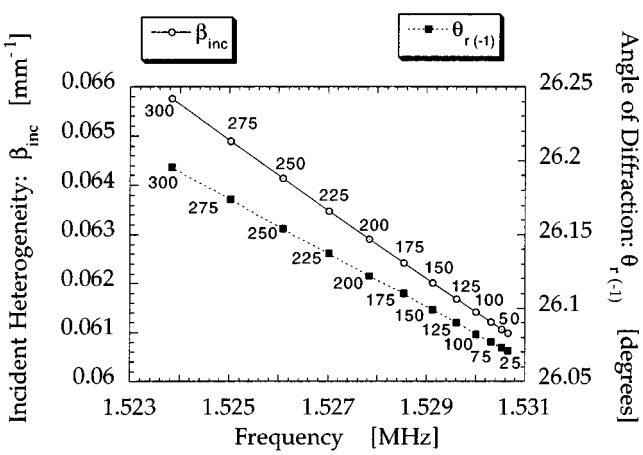

FIG. 23. Critical (f, β_{inc}) positions (full line connected circles) for the stimulation of the A_1 Lamb mode in the -1st diffraction order at normal incidence as a function of the corrugation height (25 μm$\leqslant h\leqslant$300 μm) in the case of a brass plate with a sawtooth corrugated upper surface (d=2.0 mm, Λ=2.2 mm). The dashed line connected filled squares illustrate the change in emission angle (-1st-order diffraction angle) due to the variation in corrugation height.

dence relation: Consider two solid plates of the same material with similar corrugated surfaces and with uniformly scaled dimensions: plate 1 is characterized by h_1, Λ_1, and d_1 and plate 2 is characterized by αh_1, $\alpha\Lambda_1$, and αd_1. Under these circumstances it is straightforward to prove that both plates have the same mode structure, scaled by the parameter α, i.e., resonances occurring at frequency f and heterogeneity β_{inc} on sample 1 will take place in sample 2 at frequency f/α and heterogeneity $\beta_{\text{inc}}/\alpha$. This result can be very interesting for applications such as acoustic microscopy and for NDE laboratory research on scaled models, for instance in relation to the study of ice dendrites formed by frozen seawater in the Arctic or to the investigation of the Earth's crust.

In the following section we briefly indicate the importance of the inhomogeneous wave theory on the description of bounded beam scattering on periodic surfaces. Going into more detail would require us to another full manuscript.

IV. APPLICATION TO BOUNDED BEAMS

In previous work[7,8] we reported the use of the inhomogeneous plane-wave theory in the investigation of reflection and transmission of bounded Gaussian beams. We showed that a bounded beam profile can be decomposed into a finite number of complex harmonic waves and that reflected and transmitted fields can be obtained by multiplying each inhomogeneous wave in the decomposition by its reflection/transmission coefficient. The differences with Fourier theory are that a *finite* number of *inhomogeneous* waves is used in the decomposition and that all components are propagating in the *same* direction. We studied the reflection and transmission of Gaussian beams on layered media with plane parallel interfaces using this alternative description and noted that the theoretical description of the scattered fields in reflection and transmission can be split into two components, one describing the deformed profile, and the other providing additional information about the generated leaky surface wave. The profiles are in good agreement with the results from Fourier theory. However, the great advantage of using an inhomogeneous wave decomposition is that nonspecular reflectivity of ultrasonic bounded beams is explicitly brought into close connection to the generation/stimulation of eigenmodes in the studied structure. Certain inhomogeneous waves are filtered out of the decomposition of the incident beam, which result in a deformation of the profile and a stimulation of a particular vibration mode.

Just like in the case of a smooth plate, one can apply the inhomogeneous plane-wave theory to predict the scattering of a Gaussian beam in the specular reflection and transmission direction. It is not our intention to go into details, but we would like to point out some interesting features about bounded beam scattering that can be explained using the alternative inhomogeneous plane-wave description.

As indicated in our previous publications,[7] inhomogeneous waves with both positive and negative heterogeneity coefficients are used in the decomposition of a Gaussian beam. From both theoretical and physical points of view it is straightforward to show that the reflection coefficients for any plane wave normally incident on a symmetrically corrugated surface satisfy following symmetry relations: $R_m(\beta_{\text{inc}})=R_{-m}(-\beta_{\text{inc}})$ for $m=0,1,2,3,4,...$ (and similarly for transmission). Because of this symmetry property the reflected and transmitted profiles of a symmetric incident bounded beam will be symmetric as well. Furthermore, if a Lamb wave is generated in one direction, the same Lamb wave will also be generated in opposite direction. In general, this means that four leaking trailing fields can be observed (two in reflection and two in transmission). The big difference with the case of plane parallel plates using oblique incident bounded beams is that the leaking trailing field of the generated surface wave now does not have the same direction as the R_0 reflected or T_0 transmitted wave (which is normal to the surface in the case studied here). The radiation of the stimulated Lamb wave into the surrounding liquid occurs at the specific Lamb angle, which coincides with the direction of one of the diffracted orders. The physical scattering process can thus be interpreted as follows: Certain inhomogeneous waves are filtered out of the decomposition of the incident Gaussian beam evoking a symmetrical deformation in the specular reflected and transmitted fields and creating at the same time the particular leaky plate mode in both directions inside the plate that radiate into the liquid at its characteristic critical angle in four directions.

Another interesting result mentioned in Ref. 8 is the fact that one can actually predict the optimum beamwidth required for strong generation of plate/interface modes. In the decomposition of an incident Gaussian beam of (half-)width W, the inhomogeneous wave with heterogeneity parameter $\beta_{\text{inc}}^{\max}=2.63/\text{W}$ corresponds to the component with the highest amplitude. If we now choose the beamwidth W of the Gaussian profile so that $\beta_{\text{inc}}^{\max}$ coincides with the required heterogeneity for maximum stimulation of a particular resonance at that frequency, we have created an advantageous condition for extreme generation of that leaky surface wave. For instance in the case of the sawtooth corrugated 2-mm-thick brass plate considered in Sec. I B we predict that a Gaussian beam should have a beamwidth W of about 43 mm in order to obtain efficient generation of the A_1 mode at 1.53 MHz. Under these conditions we will also observe the most intense leaking fields in plus and minus first diffraction orders. The determination of the optimum beamwidth for strong generation of plate/interface modes from a corrugated surface can be very important in NDT applications where large distances perpendicular to the surface inside a medium need to be scanned, or when large amplitude surface waves are sought in order to study nonlinear effects using eigenmodes.

Since the heterogeneity coefficients of the complex harmonic waves in the decomposition of a Gaussian beam are all inverse proportional to the width of the bounded beam, we can easily translate the independence relations for inhomogeneous plane waves, which we discussed in the last paragraph of Sec. III for the case of bounded beams. Suppose one needs to investigate the scattering of a bounded beam of width W at frequency f from a solid corrugated plate characterized by d, Λ, and h. If the dimensions of the sample are not favorable to work with (too large or too small) one can rescale the problem uniformly to laboratory proportions by a parameter α and work with a plate of identical material com-

position only now characterized by αd, $\alpha\Lambda$, and αh. Assuming that attenuation is small or proportional to frequency, resonances occurring at frequency f and beamwidth W in the unscaled sample will take place in the laboratory scaled sample at a frequency f/α and a beamwidth αW. As mentioned before, this result can be very interesting for applications such as acoustic microscopy and for NDE laboratory research on scaled models.

The last remark about bounded beam scattering deals with the double mode appearance at a single frequency. As we discussed in Sec. II about the scattering on corrugated half-spaces, stainless steel has the peculiar property that the resonance frequency for the mth order Rayleigh wave coincides with the resonance frequency for the $2m$th order Stoneley wave. We also showed that the stimulation of the Rayleigh wave and the Stoneley wave occurs for different values of incident heterogeneity. This has considerable consequences for bounded beam scattering at these double mode frequencies. If the beamwidth is such that the heterogeneity of one of the complex harmonic waves in the decomposition is close to the heterogeneity required to stimulate the Rayleigh wave, then both Rayleigh and Stoneley will be stimulated and their leaking fields will be observable in the $\pm m$th order (=Rayleigh angle) and $\pm 2m$th order (=90°). The specularly reflected and transmitted profiles will be deformed as the result of the filtering of both surface waves. The Stoneley wave effect will always be present because the homogeneous wave is always part of the decomposition of a Gaussian beam profile. However, as to the effect of the Rayleigh wave, this will depend on the beamwidth and in particular on the relative proximity of $\beta_{\text{inc}}^{\max}(=2.63/\text{W})$ to the characteristic β_{inc} that is required to stimulate the Rayleigh wave at that frequency. Another example of a possible multiple mode generation by a bounded beam can be found by looking once more at Fig. 6 in the neighborhood of 2.67-MHz frequency. At that frequency, we observe three candidate modes: the Stoneley wave can be stimulated in fourth order, the symmetrical S_1 Lamb wave can be generated in second order and the symmetrical S_3 Lamb mode can be evoked in the first diffraction order. Again, these modes correspond to different requirements for the heterogeneity coefficients. Depending on the beamwidth of the scanning wave, they may show up separately or in combinations. They will interfere inside the plate, but will radiate (to both sides of the normal) into leaking fields with different far-field directions.

V. BACKSCATTERING: AN ALTERNATIVE DESCRIPTION

In this paragraph we would like to launch an alternative concept for the physical mechanism that leads to the observation of backscattering (backreflection and backtransmission) when bounded beams interact with plane parallel plates. Some examples of experimental measurements illustrating this feature can be found in Refs. 16–19. Evidently, the backscattering is largest at the critical angles (Lamb or Rayleigh angles). However, using classical reflection and transmission theory for plane parallel interfaces, there is absolutely no way to account for waves that propagate in a direction opposite to the incident beam. On the other hand, we know that a plate (or interface) mode is stimulated when a bounded beam is incident at each of those critical angles. The interpretation in terms of the alternative bounded beam description by inhomogeneous plane waves is that some inhomogeneous waves are filtered out of the ''spectrum'' and stimulate a plate/surface wave, while the others interfere to create the specular reflected and transmitted fields. This description is probably only partly correct. The existence of a plate or surface wave in the solid medium implies that the interface between the liquid and the solid medium becomes corrugated. The corrugation periodicity is given by the wavelength of the Lamb or Rayleigh wave that has been stimulated, which corresponds to the projection of the wavelength of the incident beam onto the surface. The height of the corrugation depends on the amplitude of the incident beam, on the beamwidth and the angle of incidence. In addition, the grating is moving along the surface with the same frequency as the incident beam and is damped exponentially in amplitude because of ''reradiation.'' Since a grating is established at the interface, the bounded beam (represented by a number of inhomogeneous plane waves) will scatter into different diffracted orders. The fact that a grating is produced by a propagating wave and/or is damped exponentially does not overrule the scattering principle. On one hand, the directions of the scattered waves can be obtained by studying the generalized laws of Snell for corrugated surfaces, exactly as done in the stationary case. On the other hand, a different frequency shift per component is induced due to the Doppler effect of the moving character of the grating. (We do not take into account the fact that the amplitude of the grating is decaying exponentially.) In the case of a ''propagating'' surface grating generated by an inhomogeneous wave incident in a certain direction, one can easily verify that the minus second-order scattered component (i.e., R_{-2} and T_{-2}) of any plane-wave incident in the same direction is the only component with the same frequency as the incident wave and that this component propagates in a mirroring direction of the specular R_0 and T_0 fields with respect to the normal on the interface (i.e., exactly opposite to the incident wave in reflection). All other diffracted components are scattered in different directions and have frequencies that are multiples of the frequency of the incident wave. The idea is thus that the backreflected and backtransmitted fields exactly correspond to the -2nd-order diffracted fields of the (inhomogeneous waves that build up the) bounded beam. These fields are produced by scattering off the surface corrugation that has been created by those inhomogeneous waves in the decomposition with characteristics that are close to the resonance requirements. In this context, it is obvious that backscattering is primarily observed in the proximity of resonance conditions: the corrugation height is only large enough to produce scattering at the critical angles where Lamb or Rayleigh waves are stimulated. In addition, this interpretation leads to a better understanding of the role of the beamwidth on the backscattering intensity. From a theoretical point of view, the beamwidth determines the nature of the inhomogeneous waves in its decomposition. Depending on the heterogeneity coefficients involved in the decomposition and on the locality of the characteristic Lamb or Rayleigh heterogeneity in

this arrangement, the resonance conditions will be either more or less favorable. This means that the height of the surface corrugation will strongly depend on the beamwidth of the incident beam, and as a consequence also the backscattering itself.

So far, this alternative concept of backscattering is only qualitative. We hope to develop a more quantitative model that includes intensity predictions in the near future.

VI. CONCLUSION

We illustrated that, in general, only complex harmonic waves can stimulate eigenvibrations of structures with either smooth parallel interfaces or periodic corrugated rough surfaces. It was shown that the location of the modes for a corrugated specimen can be deduced from the dispersion curves of a sample with plane parallel interfaces. Examples are provided showing the influence of sample thickness, corrugation profile, height, and periodicity on the characteristics of a particular mode.

Qualitatively we applied the complex harmonic wave reflection and transmission properties to examine the deformation of Gaussian profiles on periodic rough surfaces at normal incidence. Doing this, one can explicitly link the beam deformation to the stimulation of mode vibrations. Symmetry properties, beamwidth influence, and multiple mode occurrence can all be interpreted in a meaningful way in terms of complex harmonic waves.

We also showed that the determination of the required heterogeneity coefficient of a mode stimulating inhomogeneous wave is necessary for the prediction of the optimum beamwidth when seeking strong plate/surface wave generation using bounded beam scattering on periodic rough surfaces. These high amplitude eigenmodes can be used in linear and nonlinear NDT applications.

We also discussed an alternative approach of backscattering by combining inhomogeneous wave mode stimulation and scattering from periodic corrugated surfaces. Backreflection and backtransmission correspond to the -2nd diffraction order of a bounded beam scattered from the moving corrugated surface that it created itself. Near resonance this corrugation is largest which explains why backscattering is primarily observed at critical angles. The inhomogeneous wave theory also provided a plausible explanation for the beamwidth dependence of the backscattering.

ACKNOWLEDGMENTS

This research is supported by the Belgian National Fund for Scientific Research and the Office of Basic Energy Science, Engineering and Geoscience in cooperation with Los Alamos National Laboratory.

[1] B. Poirée, ''Les Ondes Planes Evanescentes dans les Fluides Parfaits et les Solides Elastiques,'' J. Acoust. **2**, 205–216 (1989).
[2] B. Poirée, ''Complex Harmonic Waves,'' in *Proceedings of the Symposium on Physical Acoustics: Fundamentals and Applications*, Kortrijk, Belgium, edited by O. Leroy and M. Breazeale (Plenum, New York, 1990), pp. 99–117.
[3] M. Deschamps, ''L'Onde Plane Hétérogène et ses Applications en Acoustique Linéaire,'' J. Acoust. **4**, 269–305 (1991).
[4] I. A. Viktorov, *Rayleigh and Lamb Waves: Physical Theory and Applications* (Plenum, New York, 1967).
[5] G. C. Bishop and J. Smith. ''A Scattering Model for Nondifferentiable Periodic Surface Roughness,'' J. Acoust. Soc. Am. **91**, 744–770 (1992).
[6] D. Maystre, *Selected Papers on Diffraction Gratings*, SPIE Milestone Series Vol. MS 83 (SPIE, Washington DC, 1993).
[7] K. Van Den Abeele and O. Leroy, ''Complex Harmonic Wave Scattering as the Framework for Investigation of Bounded Beam Reflection and Transmission at Plane Interfaces and its Importance in the Study of Vibrational Modes,'' J. Acoust. Soc. Am. **93**, 308–323 (1993).
[8] K. Van Den Abeele and O. Leroy, ''On the Influence of Frequency and Width of an Ultrasonic Bounded Beam in the Investigation of Materials: Study in Terms of Heterogeneous Plane Waves,'' J. Acoust. Soc. Am. **93**, 2688–2699 (1993).
[9] M. Deschamps, ''Reflection of the evanescent plane wave on a plane interface,'' J. Acoust. Soc. Am. **96**, 2841–2848 (1994).
[10] J. W. Stutt (Lord Rayleigh), *The Theory of Sound* (Dover, New York, 1945), Vol. 2, Sec. 272a, pp. 89–96.
[11] L. N. Deryugin, ''Equations for the Coefficients of Reflection of Waves from Periodically Uneven Surfaces,'' Dokl. Acad. Nauk. SSSR **87**, 913–916 (1952).
[12] B. A. Lippman, ''Note on the Theory of Gratings,'' J. Opt. Soc. Am. **43**, 408 (1953).
[13] R. F. Millar, ''The Rayleigh Hypothesis and a Related Least-Squares Solution to Scattering Problems for Periodic Surfaces and Other Scatterers,'' Radio Sci. **8**, 785–796 (1973).
[14] A. Wirgin, ''Reflection from a corrugated surface,'' J. Acoust. Soc. Am. **68**, 692–699 (1980).
[15] J. A. DeSanto, ''Scattering from a Periodic Corrugated Structure: Thin Comb with Soft Boundaries,'' J. Math Phys. **12**, 1913–1921 (1971).
[16] S. Sasaki, ''Back Reflection of Ultrasonic Waves Obliquely Incident to a Solid Surface in Water,'' Jpn. J. Appl. Phys. **2**, 198 (1963).
[17] W. G. Neubauer, in *Elastic Wave Scattering and Propagation*, edited by V. K. Varadan and V. V. Varadan (Ann Arbor Science, Ann Arbor, MI, 1982).
[18] M. de Billy, L. Adler, and G. Quentin, ''Parameters affecting Backscattered Ultrasonic Leaky-Rayleigh Waves from Liquid–Solid Interfaces,'' J. Acoust. Soc. Am. **72**, 1018–1020 (1982).
[19] I. Molinero, ''Contribution à l'Etude de la Diffusion Acoustique par des Plaques et des Fils en Incidence Oblique; Génération d'Ondes de Surface et d'Ondes Guidées,'' Ph.D. thesis, Université Paris VII, France (1987); I. Molinero, M. de Billy, and G. Quentin, ''Experimental Investigation of the Resonant Behavior of the Transmission Coefficient of a Fluid-Loaded Elastic Plate,'' in *Proceedings of Ultrasonics International '87* (Butterworth–Heinemann, London, 1987), pp. 629–634.
[20] L. M. Brekhovskikh, *Waves in Layered Media* (Academic, New York, 1960).
[21] W. M. Ewing and W. S. Jardetzky, *Elastic Waves in Layered Media* (McGraw-Hill, New York, 1957).
[22] R. Briers and O. Leroy, ''Reflection of Inhomogeneous Plane Ultrasonic Waves on Periodically Rough Solid–Vacuum Interfaces,'' in *Proceedings of the 5th Spring-School on Acousto-Optics and Applications*, edited by A. Sliwinski (SPIE, Washington, DC, 1992).
[23] W. Huang, R. Briers, S. I. Rokhlin, and O. Leroy, ''Experimental study of inhomogeneous wave reflection from a solid–air periodically rough boundary using leaky Rayleigh waves,'' J. Acoust. Soc. Am. **96**, 363–369 (1994).
[24] J. M. Claeys, O. Leroy, A. Jungman, and L. Adler, ''Diffraction of Ultrasonic Waves from Periodically Rough Liquid–Solid Surface,'' J. Appl. Phys. **54**, 5657–5662 (1983).
[25] K. Mampaert and O. Leroy, ''Reflection and Transmission of Normally Incident Ultrasonic Waves on Periodic Solid–Liquid Interfaces,'' J. Acoust. Soc. Am. **83**, 1390–1398 (1988).